

## Retraction

# Retracted: Dance Movement Interference Suppression Algorithm Based upon Contour Model and AdaBoost Algorithm

### Journal of Electrical and Computer Engineering

Received 15 August 2023; Accepted 15 August 2023; Published 16 August 2023

Copyright © 2023 Journal of Electrical and Computer Engineering. This is an open access article distributed under the Creative Commons Attribution License, which permits unrestricted use, distribution, and reproduction in any medium, provided the original work is properly cited.

This article has been retracted by Hindawi following an investigation undertaken by the publisher [1]. This investigation has uncovered evidence of one or more of the following indicators of systematic manipulation of the publication process:

- (1) Discrepancies in scope
- (2) Discrepancies in the description of the research reported
- (3) Discrepancies between the availability of data and the research described
- (4) Inappropriate citations
- (5) Incoherent, meaningless and/or irrelevant content included in the article
- (6) Peer-review manipulation

The presence of these indicators undermines our confidence in the integrity of the article's content and we cannot, therefore, vouch for its reliability. Please note that this notice is intended solely to alert readers that the content of this article is unreliable. We have not investigated whether authors were aware of or involved in the systematic manipulation of the publication process.

Wiley and Hindawi regrets that the usual quality checks did not identify these issues before publication and have since put additional measures in place to safeguard research integrity.

We wish to credit our own Research Integrity and Research Publishing teams and anonymous and named external researchers and research integrity experts for contributing to this investigation.

The corresponding author, as the representative of all authors, has been given the opportunity to register their agreement or disagreement to this retraction. We have kept a record of any response received.

### References

- [1] J. Xu, "Dance Movement Interference Suppression Algorithm Based upon Contour Model and AdaBoost Algorithm," *Journal of Electrical and Computer Engineering*, vol. 2022, Article ID 3998449, 11 pages, 2022.

## Research Article

# Dance Movement Interference Suppression Algorithm Based upon Contour Model and AdaBoost Algorithm

Jiayi Xu 

*The Faculty of Physical Education, Chongqing Jiaotong University, Chongqing 400074, China*

Correspondence should be addressed to Jiayi Xu; 990201900060@cqjtu.edu.cn

Received 5 March 2022; Revised 25 April 2022; Accepted 3 May 2022; Published 2 June 2022

Academic Editor: Wei Liu

Copyright © 2022 Jiayi Xu. This is an open access article distributed under the Creative Commons Attribution License, which permits unrestricted use, distribution, and reproduction in any medium, provided the original work is properly cited.

With the development of computer technology, digital image processing, as an emerging field, has become an indispensable tool in the information society. The action interference effect refers to the phenomenon that an individual reacts to a dangerous object longer than a safe object in the state of preparation for action. Currently, there is no effective anti-jamming technology to recognize dance movements. In order to solve these problems, this paper proposes a dance movement interference suppression algorithm based on contour model and AdaBoost algorithm, which aims to realize the application of gesture-based behavior recognition technology in the field of dance steps and complete the recognition of some dance steps. The method of this paper is to study the contour model based on the image and then propose to use the AdaBoost algorithm to detect body movements and finally use the radio frequency interference suppression algorithm to ensure the smooth operation of the technology. The function of the method is to propose a dance action recognition and anti-interference algorithm based on contour model and AdaBoost algorithm. This article describes the contour model and then uses the AdaBoost algorithm to recognize the action and adjust the action interference effect. The results show that the algorithm proposed in this paper can accurately identify dance movements, with an average recognition accuracy rate of 99.2%.

## 1. Introduction

In the recent video action recognition research process, the main types of action video include daily human behaviors such as walking, running, waving, and clapping, as well as sports such as diving, skating, and horse riding. There are also life activities, such as cooking and washing dishes. Among the many researches on human movement recognition, many organizations choose to study dance movements. The main reason is that dance is a way of expressing emotions to the public through body movements, and there is almost no corresponding research in this field. The dance moves also include many unique dance steps. Therefore, the current academic research on dance moves is still in the stage of dance step analysis. In most cases, this article will analyze the collected dance movements and apply them to the performance of animated characters using animation processing software.

This article focuses on the key technology of intelligent video surveillance dance movements. The research content

of this paper includes moving object detection, interpretation of human motion characteristics, recognition methods, and so on. The research in this article has specific theoretical research value and practical application importance. Image acquisition equipment can complete recognition tasks, greatly improving the versatility and practicability of motion recognition, video surveillance, video search, video coding, human-computer interaction, medical treatment, sports, and other fields. Faced with a kind of intangible cultural heritage that is constantly disappearing due to lack of heirs, this article uses motion recognition technology to provide information on important human actions in order to achieve the purpose of inheriting behaviors related to intangible cultural heritage. In many places in China, there are dances with ethnic characteristics. Motion recognition technology captures and stores important information about dance movements, reducing the possibility of interruption in dance inheritance.

This dissertation focuses on the rapid acquisition and anti-interference of video receiver signals and aims to

improve receiver performance and reduce processing complexity. Starting from the top-level module, this paper merges the transform domain interference suppression algorithm and the frequency domain parallel acquisition algorithm, and applies the latest theory of sparse signal processing. This paper proposes to combine the cascaded interference suppression algorithm and the acquisition algorithm into one. By realizing interference suppression and acquisition processing at the same time for forward and backward FFT operations, this paper reduces the signal processing complexity of the receiver by a factor of one. This paper simplifies the calculation of IFFT in the joint algorithm based on the sparse Fourier transform and reduces the computational complexity from the  $O(n \log n)$  level to the sub-linear level. Compared with traditional motion recognition using contact sensors (3D speed sensors, EMG signal sensors, etc.), the computer vision-based human motion recognition proposed in this paper is the object of collaborative analysis under laboratory conditions and does not require sensor contact.

## 2. Related Work

As the contour model and AdaBoost algorithm become more mature, people have used these technologies in many fields. In order to deal with the poor boundaries of noise and magnetic resonance image heterogeneity, Alipour N proposed an active contour model for brain tumor segmentation surgery. He uses superpixels as the basic atomic unit, which not only reduces the sensitivity to the factors, but also reduces the computational cost of the algorithm [1]. Yang constructed a new level set algorithm based on nonlocal mean filtering. He first performs nonlocal mean filtering on the image to generate an edge map. The new edge stop function and fuzzy k-NN classification algorithm constructed from the edge map are incorporated into the variational model. His experiments show that nonlocal mean filtering can sharpen edges on medical and natural images [2]. Feng proposed a bias-corrected embedded level set model, in which the inhomogeneity is estimated by orthogonal main functions. He extended the proposed model to multi-channel and multi-phase modes to separate color images and images with multiple objects [3]. Zhao proposed a method to complete face detection and human tracking. He proposed a method that combines the face detection algorithm based on AdaBoost and the target tracking method based on Kalman filter [4]. Liu proposed an early termination algorithm based on the AdaBoost coding unit classifier to speed up the process of searching for the best CTU partition. His method takes the Bjontegaard delta rate increase by 0.18 as the cost, which can save an average of 39% of the computational complexity [5]. Yang uses the improved AdaBoost-SVM algorithm to classify the security and risk of online lending platforms. His experimental results show that the AdaBoost algorithm can improve the accuracy of risk platform classification, and the calculated error rate is only 5% [6]. Yang integrates the skin color model and the improved AdaBoost algorithm into a face detection method for high-resolution images with complex backgrounds [7].

## 3. Contour Model and AdaBoost Algorithm Research Method

**3.1. Image-Based Contour Model.** In recent years, GACM has been widely used in image segmentation. This method first creates a contour expansion curve and assigns an energy function to the curve, and then uses the geometry of the image to minimize the energy function and make the development curve closer to the target boundary of the image. Through the analysis of geodesic active contour model and CV model, the active contour model proposed in this paper includes edge detection coefficients. This model can effectively solve the segmentation problem of images containing nonuniform regions, but many image attributes in the model are calculated and controlled by constraints. This complicates the calculation of the model, and the segmentation result is highly dependent on the size of the evolution curve and the choice of initial position. The C-V model can improve the accuracy of curve expansion in the presence of occlusion and severe edge noise. It is not affected by the initial position and is easy to calculate. However, for images that contain uneven areas, the segmentation effect is not enough. Based on the considerations, this paper proposes a hybrid GACV model with adaptive characteristics based on the geodesic contour model and the C-V model. The proposed model reduces the interference of human factors and improves the robust performance of image segmentation. The specific model is as follows:

$$E = x \int g(|\nabla I|) dx dy + (1-x) \left( \int |\nabla I| dx dy + \int |1 - c_2|^2 dx dy \right). \quad (1)$$

Among them,  $x$  is a weight function satisfying  $x_0, 1$ . When  $x = 0$ , the model degenerates to a C-V model due to the expansion of the contour. When  $x = 1$ , the model degenerates to an active contour model due to the expansion of the contour curve. For  $x \in (0, 1)$ , both models work at the same time. This solves the problem of segmenting heterogeneous images and segmenting images with more complex edge information, which is conducive to the evolution of contour lines and realizes image segmentation [8]. So far, most of the weights have been manually selected. For this reason, in view of the characteristics of different image regions, this paper creates the following  $x$ -weighting function.

$$x = 0.5 \cos \left( \pi \frac{|\nabla I|}{225\sqrt{2}} + \pi \right) + 0.5. \quad (2)$$

When the image area shows homogeneous characteristics,  $x$  slowly approaches 0 as the  $|\nabla I|$  value decreases, and the mixed model tends to the C-V model at this time. When the image area exhibits heterogeneous or boundary characteristics,  $x$  slowly approaches 1 with the increase of  $|\nabla I|$  value. At this time, the hybrid model tends to be the geodesic active contour model. The corresponding function curve is shown in Figure 1.

The contour curve of the parametric active contour model is composed of a set of control points connected end to end in a straight line. These control points are defined as  $v(n) = [x(n), y(n)]$ ,  $n \in [0, 1]$ . Among them,  $x(n)$  and  $y(n)$  are the coordinate values of these control points, and  $n$  is the arc length of the normalized curve. The energy function of the parametric active contour model is expressed as follows:

$$E = \int \left[ a(n) \left| \frac{\partial}{\partial n} \vec{v} \right|^2 + b(n) \left| \frac{\partial^2}{\partial n^2} \vec{v} \right|^2 + E(\vec{v}(n)) \right] dn. \quad (3)$$

The  $a(n)$  and  $b(n)$  in the formula represent the slope and curvature of the curve, respectively. Using the variational method for the energy formula (3), the Euler-Lagrange formula can be expressed as follows:

$$-av'(n) + bv''(n) + \nabla E(x, y) = 0. \quad (4)$$

Regarding the deformation curve  $v(n)$  as a function of time  $f$ , formula (4) can be transformed into the following gradient descent flow formula:

$$-av'(n) + bv''(n) + \nabla E(x, y) = \frac{\partial v}{\partial t}. \quad (5)$$

Figure 2 shows a schematic diagram of target contour segmentation using a parametric active contour model, where the black points are a set of control points of the parametric active contour model, and the blue curve is the final segmentation result. It can be seen from the figure that the parameter active contour model can better extract the boundary of the target area in the image and has a good segmentation effect.

The GAC model in the form of partial differential formulas takes the following form:

$$\frac{\partial \phi}{\partial t} = g(|\nabla I|) (k + v) |\nabla \phi| + \nabla g \cdot \nabla \phi. \quad (6)$$

In the formula,  $v$  represents the constant coefficient of weight.  $k$  represents the curvature of the curve.  $\phi$  stands for level set function.  $g(|\nabla I|)$  stands for edge indicator function, which is defined as follows:

$$g(|\nabla I|) = \frac{1}{1 + |\nabla(G_Q \times I)|^2}. \quad (7)$$

$|\nabla I|$  in the formula represents the gradient of the image.  $G_Q$  represents a Gaussian convolution function with a standard deviation of  $Q$ . The M-S model aims at accurately solving the target edge; that is, the error value between the segmented image  $I_o(x, y)$  and the original image  $I(x, y)$  is smaller than the image error value obtained by other boundary segmentations. Therefore, the energy functional of the M-S model can be expressed as the following form:

$$E(C, I_o) = n \int |I - I_o|^2 dx dy + m \int |\nabla I_o|^2 dx dy + u|W|. \quad (8)$$

In the formula,  $n$ ,  $m$ , and  $u$  are all control parameters.  $|W|$  represents the length of the profile curve. This paper uses a two-phase split constant C-V model to simplify the

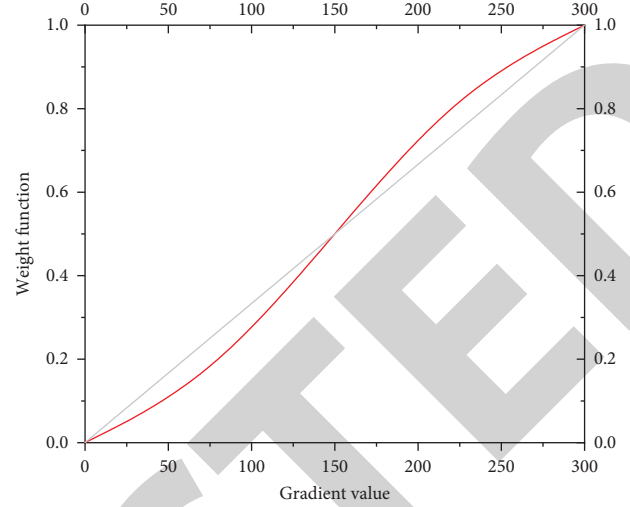


FIGURE 1: Schematic diagram of weight function curve.

M-S algorithm. The basic idea of the M-S algorithm is to assume that the grayscale distribution of the image to be segmented in the homogeneous area is a constant value. The closed curve  $c$  divides the entire image into a target area (denoted as inside (C)) and a background area (denoted as outside (C)). The energy functional of the model is defined as follows:

$$E(C, c_1, c_2) = n_1 \int |I - c_1|^2 dx dy + n_2 \int |I - c_2|^2 dx dy. \quad (9)$$

In the formula,  $n_1, n_2$  represents the weight coefficient of the energy term.  $c_1, c_2$  represents the average gray value inside and outside the contour curve, which is specifically defined as

$$c_1, c_2 = \frac{\int I(x, y) dx dy}{\int dx dy}. \quad (10)$$

Figure 3 shows a schematic diagram of the segmentation of the C-V model. The blue initial contour curve  $C$  and the black target area have the following four relationships.

**3.2. AdaBoost Algorithm Detects Body Movements.** The AdaBoost algorithm is an adaptive recommendation method. In actual work, the idea of many people is to find a weak classifier that is slightly better than random guessing, hoping to train a strong classifier. The AdaBoost algorithm is applied under this concept. The AdaBoost algorithm first marks the face samples and nonface samples, and then initializes the face samples and nonface samples separately. The reason for this is related to the actual experiment. In the experiment, the number of face samples is generally smaller than that of nonface samples. Failure to perform separate initialization processing will make nonface samples pay more attention during training, which will have a greater negative impact on the detection rate [9].

Taking a  $20 \times 20$  training sample as an example, there are 68459 Haar-like features. Assuming that the number of

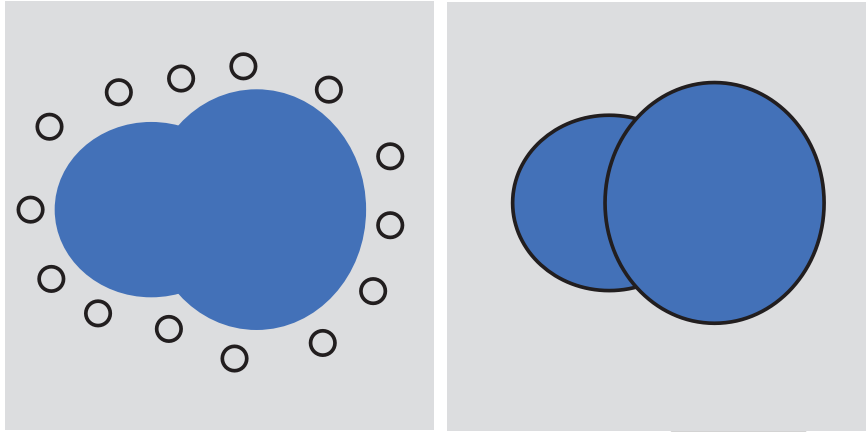


FIGURE 2: Schematic diagram of segmentation of parametric active contour model.

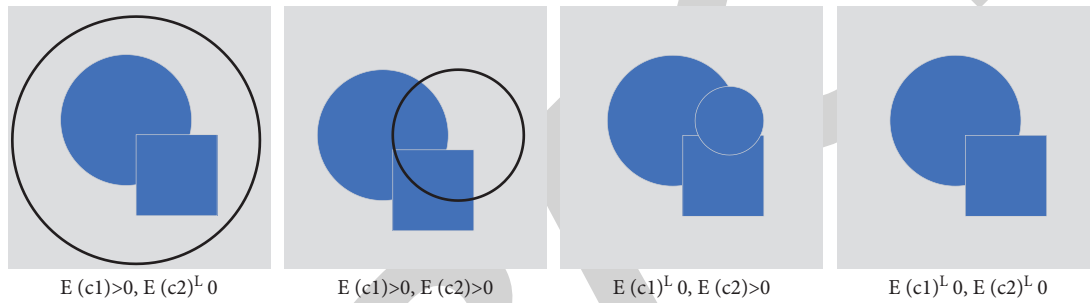


FIGURE 3: Schematic diagram of the segmentation of the C-V model.

samples is  $n$ , each round of training will find the best classifier for these 68459 features to minimize the objective function  $e_j = \sum_{i=1}^n w_{t,i} |h_j(x_i) - y_i|$ , where  $w_{t,i}$  represents the weight of the  $i$ -th sample in the  $t$  round, the calculation result of  $|h_j(x_i) - y_i|$  indicates whether the judgment of the weak classifier is correct,  $|h_j(x_i) - y_i| = 0$  indicates that the classification result is correct, and  $|h_j(x_i) - y_i| = 1$  indicates that the classification result is wrong. Updating sample weights is the focus of the AdaBoost algorithm. It is precisely because of this step that the AdaBoost algorithm values are only trained with the same sample set, and the weights are updated in each iteration. According to whether the sample classification is correct or not, the weight of the incorrectly classified sample is increased, and the weight of the correctly classified sample is relatively reduced [10].

$$w_{t+1,j} = w_{t,j} b_t^{1-e} = w_{t,j} \left( \frac{e_t}{1-e_t} \right)^{1-e}. \quad (11)$$

At this time  $w_{t+1,j} < w_{t,j}$ , the sample weight is reduced. When  $|h_j(x_i) - y_i| = 1$ ,  $e = 1$ .

$$w_{t+1,j} = w_{t,j} \left( \frac{e_t}{1-e_t} \right)^{1-e} = w_{t,j}. \quad (12)$$

Since the boosting algorithm needs to know the lower limit of the classification accuracy of the weak classifier in advance, and the lower limit is often unknown, this article uses the representative AdaBoost algorithm of the boosting algorithm family. The basic idea of the AdaBoost algorithm is to combine several different decision trees in a nonrandom way to get a powerful classifier.

Figure 4 illustrates the training process of the basic classifier of the AdaBoost algorithm. Specifically, the AdaBoost algorithm can be roughly divided into three steps.

a. Initialize the weight distribution of the training data. In other words, if there are  $N$  samples in the training set, each sample will be given the same weight. b. Basic classifier training: if a particular training sample is accurately classified in one iteration, the weight of the sample will be reduced in the next iteration. Otherwise, the weight will increase. Then, update the weights in the test sample set, train the next basic classifier, and iterate multiple times until the error rate is less than 0.5 or the maximum number of iterations is reached. c. Generate a powerful classifier. The error rate is inversely proportional to the weight of the basic classifier. Given the weight of the basic classifier, the greater the weight, the greater the decisive power of the final classification, and the greater the influence of the insufficient basic classifier. In the end, the performance of the classifier is reduced.



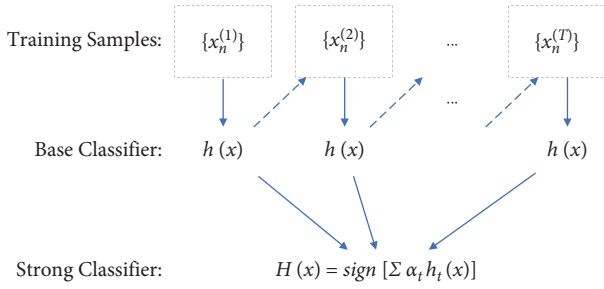


FIGURE 4: The base classifier training process of the AdaBoost algorithm.

Construct a linear combination of basic classifiers:

$$f(x) = \sum_{t=1}^T \alpha_t h_t(x). \quad (13)$$

So as to get the final classifier,

$$H(x) = \text{sign}(f(x)) = \text{sign}\left[\sum_{t=1}^T \alpha_t h_t(x)\right]. \quad (14)$$

It can be seen from formula (14) that the final classification result is jointly determined by the T-based classifier through voting, and the deterministic ability is completely determined by each a [11].

**3.3. Radio Frequency Interference Suppression Algorithm.** Aiming at the RFI problem in active high-frequency radars, anti-jamming methods include adaptive frequency selection or various space, time, and frequency domain signal processing methods [12]. Combining the system and waveform characteristics of DRM waveform high-frequency external radiation source radar, there are RFI parameter estimation method MLE based on time-domain signal processing method and subspace projection algorithm based on distance spectrum domain. The following two methods are used as examples to introduce the RFI suppression technology in high-frequency external radiator radar. Normally, let the length of the original data sequence contaminated in a symbol be  $L$ , and use  $q(n)$  to represent this original data:

$$q(n) = b_0 \exp[j(a_0 + a_1 n)] + v(n), \quad 0 \leq n \leq L-1. \quad (15)$$

Among them, RFI is represented by  $b_0 \exp[j(a_0 + a_1 n)]$ , and other components of useful echo, residual clutter, and noise are represented by  $v(n)$ . First, get the frequency spectrum of the time-domain signal, and the position of the RFI can be determined by using the peak-to-noise ratio, through a fixed threshold or constant false alarm detection [13]. When RFI is detected, interpolation and peak search can be used to obtain a rough estimate of the frequency, which is represented by  $a_1$  to compensate for this part of the interference:

$$q_1(n) = q(n) \exp[-ja_1 n] + v_1(n). \quad (16)$$

Among them, the difference between the rough estimate value and the true frequency value is represented by  $\delta a = a_1 - a_n$ . Generally speaking, it is also necessary to use the maximum likelihood algorithm to estimate the frequency precisely, because the accuracy of the rough estimate cannot meet the needs of the project. According to the maximum likelihood algorithm, it can get

$$\sum_{k=0}^{L-1} \sum_{n=0}^{L-1} n \cdot q_1(k) q_1^* \exp[-j\delta a_1(n-k)] = \delta a. \quad (17)$$

Because rough estimation and compensation were used earlier,  $|\delta a_1 M| < 1$  can be used. According to the linear approximation relationship,

$$\exp[\pm j\delta a_1(n-k)] \approx 1 \pm j\delta a_1(n-k). \quad (18)$$

Then, it can get

$$\delta a_1 \text{Re} \left\{ \sum_{k=0}^{L-1} z_1[k] \sum_{n=0}^{L-1} n^2 z_1^*[n] \right\} = \text{Im} \left\{ \sum_{k=0}^{L-1} z_1^*[k] \sum_{n=0}^{L-1} n z_1^*[n] \right\}. \quad (19)$$

The real part and imaginary part of the complex number are represented by Re and Im, respectively. Substitute  $\delta a_1$  to obtain the estimated values of  $b_0$  and  $a_0$ . The data after the final removal of RFI can be expressed by

$$q(n) = q[n] - b_0 \exp[j(a_0 + (a_1 + \delta a_1)n)]. \quad (20)$$

This article can also use multiple iterations to improve the robustness of the algorithm, because sometimes there may be multiple interference sources or residual interference introduced due to model errors and estimation accuracy [14]. The specific algorithm process is shown in Figure 5.

Combined with the analysis of the characteristics of radio frequency interference on the two-dimensional spectrogram of high-frequency external radiation source radar, this paper proposes an image processing-based radio frequency interference detection and suppression method based on the research of existing signal processing radio frequency interference suppression algorithms.

## 4. Dance Action Recognition Experiment and Analysis

**4.1. Outline Model Description Method.** The human body model refers to the posture represented by the structure of the human body. The description method based on the human body model essentially parameterizes the human body and its posture, and recognizes human behavior by analyzing these parameterized human body models. Compared with low-level image information, it can describe human behavior in more detail. According to the different human body models used in the feature extraction process, this behavior description method can be divided into three types: line drawing model, 2D contour model, and 3D contour model. Line drawing models and two-dimensional models are used for human behavior and are widely used to recognize human behavior. Although the 3D model can

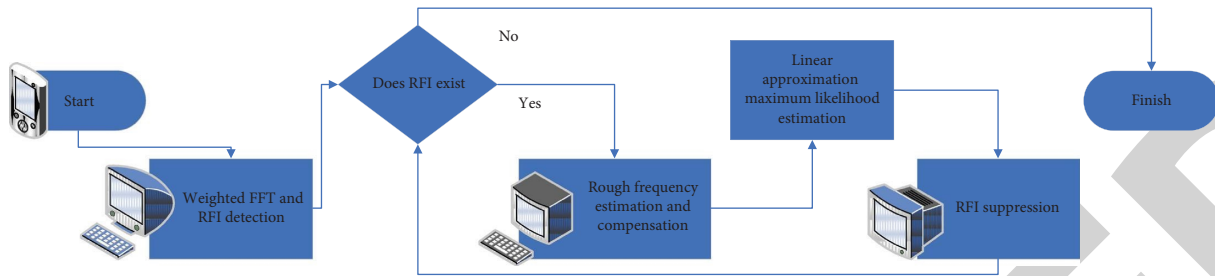


FIGURE 5: RFI suppression algorithm flowchart.

represent the posture of the human body more accurately, it is not often used for human behavior recognition due to its high complexity and difficult parameter estimation [15].

The two-dimensional contour human body model is a common model for human body detection and tracking. This method is related to the projection of the human body in the image, and the outline formed by the projection of the human body is used to represent the human body. In many cases, users can use moving object detection techniques (such as background subtraction) to segment and segment moving objects from video frames to extract their contours. On this basis, the human body contour model is used to determine whether the target is a human body, and its posture is further analyzed. In this article, the 2D contour model in Figure 6 will be used to analyze the posture of the human body in the gymnastics sequence.

The contour area represents a specific part of the human body. There are a total of five U-shaped belt-shaped regions in the model used to construct the human body. The five areas from A to E represent the head and limbs of the human body. This model can segment the human body contour, describe each part of the human body, locate the joint points of the human body, and finally get the description of the human body's dance posture and movement [16]. In order to extract key frames, the cost function between the contour curves is calculated, and the distance matrix of each behavior is obtained. Table 1 shows the distance matrix formed by the distances between the six typical pose contours.

There are 6 cognitive experiments in total, each experiment takes 6 actions, and the number of experiments is 40. Table 2 shows the correct recognition rate, false recognition rate, and rejection rate.

In general, the algorithm has a high recognition rate for six simple dance moves. The recognition rate of raising hands is the highest, and the recognition rate of clapping hands is low [17]. This is mainly because the recognition method used in this article is based on the human shape features of the action sequence. If these two actions resemble the shape of a human body, it is easy to misunderstand.

#### 4.2. Action Recognition Based on AdaBoost Algorithm.

The AdaBoost algorithm was first applied to recognize handwritten fonts, and it is also the most successful and practical application of the algorithm. The algorithm not only significantly reduces the recognition error rate, but also recognizes different types of fonts. This article introduces the

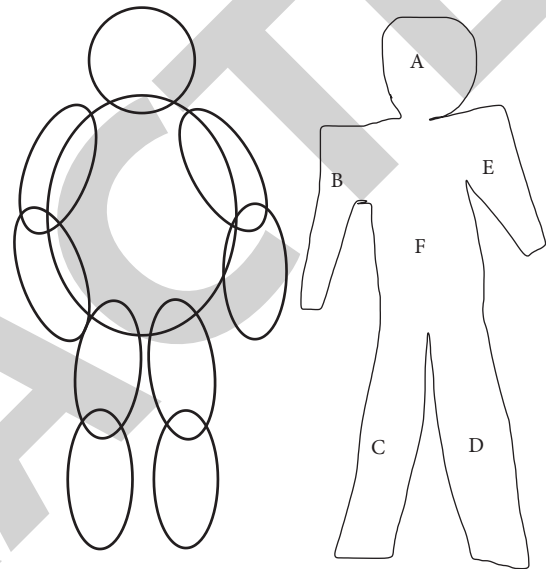


FIGURE 6: Two-dimensional human contour model.

application of AdaBoost algorithm in the field of motion recognition. Before the pattern recognition experiment, this article will conduct neural network training on the surface EMG signals collected by the tester [18]. In this training, 100 sets of signals were collected for each action, including 60 sets for normal and 40 sets for fatigue. According to Table 3 60 groups of normal surface EMG signals were assigned. Each time the neural network is trained, 15–35 of the 60 groups in the total sample are randomly selected as the training set, and the remaining 50 groups are used as the test set.

The surface EMG signal is a signal with small amplitude, nonstationary, and easily affected by external noise. How to select the characteristics suitable for the processed EMG signal is the key to hand movement pattern recognition. Feature extraction is the first step in action pattern recognition, and it is also the basis for achieving a good pattern recognition effect. The selection of features should be selected according to the changes in the characteristics of the input signal, and different features are suitable for different signal conditions. Because the collected signal data are too much and contain many features, it is indistinguishable just by observation. The purpose of feature extraction is to find out the main information containing EMG signal through selection and experiment. And it can

TABLE 1: Distance matrix of six typical poses.

Posture	Bending	Stretch	Go round	Slap	Raise your foot	Raise hand
Bending	0	—	—	—	—	—
Stretch	0.48	0	—	—	—	—
Go round	0.29	0.21	0	—	—	—
Slap	0.36	0.48	0.21	0	—	—
Raise your foot	0.25	0.21	0.4	0.25	0	—
Raise hand	0.42	0.39	0.29	0.49	0.23	0

TABLE 2: Six types of behavior recognition results.

	Accuracy (%)	False recognition rate (%)	Rejection rate (%)
Bending	90.28 ± 3.48	85.51 ± 0.74	91.6 ± 1.51
Stretch	89.4 ± 2.52	91 ± 4.25	94.94 ± 1.94
Go round	90.21 ± 3.53	91.79 ± 1.69	93.78 ± 4.28
Slap	88.98 ± 4.43	94.7 ± 4.47	85.6 ± 2.69
Raise your foot	86.91 ± 0.56	89.15 ± 2.08	93.97 ± 3.56
Raise hand	90.39 ± 2.64	85.9 ± 3.62	88.24 ± 3.57

TABLE 3: Groups of surface EMG signals under normal conditions.

Action	Number of training samples	Number of test samples
Make a fist	20	50
Palm valgus	15	50
Palm inversion	20	50
Gesture	35	50

best be used to distinguish the features of actions, thereby reducing the number of distinguishing features, reducing the difficulty of classification and the amount of calculation, and at the same time ensuring the accuracy and stability of classification.

It can be seen from Figure 7 that the recognition rate of each action basically increases as the number of hidden layer nodes increases. But when the hidden layer is greater than 6, the growth rate remains basically stable, the difference is not much, and the more the hidden layer nodes, the more complex the network, it is easy to over-iterate, but affects the classification effect. In contrast, when the number of hidden layer nodes is 6, the relative classification effect of the four actions is the best.

This paper uses the AdaBoost algorithm to classify multiple weak classifiers and a BP neural network to form a strong classifier. The number of weak classifiers varies according to different situations. In this paper, the number of weak classifiers is set to 3, 4, 5, 6, 7, 8, and 9, respectively, and four kinds of behavior recognition rates are calculated [19]. The selected weak classifier is the BP neural network, and the initial settings are performed according to the BP neural network. The experiment is carried out for 20 iterations. By calculating the average value, the recognition rate of the four actions with different numbers of weak classifiers is shown in Figure 8.

This section uses STIP's BoW histogram and NN classifier for action recognition. For fair comparison, the size of

the training set is  $11 \times 25 \times 100$ , and the STIP is clustered using a merge algorithm based on "full connection." Figure 9 shows the performance of BoW recognition under different codebook sizes.

The AdaBoost algorithm is compared with 6 BP neural networks as weak classifiers, and the absolute error value is the absolute value of the difference between the training output value and the target value. As shown in Figure 9, the horizontal axis is 80 samples, and the absolute value of the error of the 80 samples on the vertical axis. (a) is the fist, and (b) is the flip of the palm. The red circle line represents the average of the six BP neural network errors, and the blue triangle line represents the error value of the AdaBoost algorithm. This shows that the output value after the AdaBoost algorithm is closer to the target classification value, and is more accurate, and the result is more stable. This paper has completed the experiment and analysis of surface EMG signal pattern recognition [20]. For the four actions selected in this article, this article will compare the influence of the number of hidden layer nodes on the recognition rate of BP neural network. This paper chooses the appropriate number of nodes to configure the BP neural network, as well as the various weaknesses of AdaBoost, and calculates the classifier, recognition rate, and iteration time of the two algorithms for surface EMG signals. It analyzes the recognition rate and effect of AdaBoost algorithm under fatigue EMG signal interference. Experiments show that the AdaBoost algorithm improves the recognition ability of surface EMG signals. According to the data in Figure 8, the average recognition rate of the algorithm reaches 99.2%.

#### 4.3. The Moderating Effect of Action Interference Effects.

In order to verify the effectiveness and superior performance of the iterative method for wideband interference suppression in the low spread spectrum gain system, fixed-point simulations are carried out. The fixed-point simulation parameters of the broadband digital interference scene are shown in Table 4.

This chapter will introduce in detail the implementation and verification of interference suppression technology in low spread spectrum gain systems. First of all, this article presents the demand analysis of the low spread spectrum gain system interference suppression verification platform, including the overall structure of the verification platform, the functional requirements and performance requirements of the transmitter, and the functional requirements and performance requirements of the receiver. Secondly,



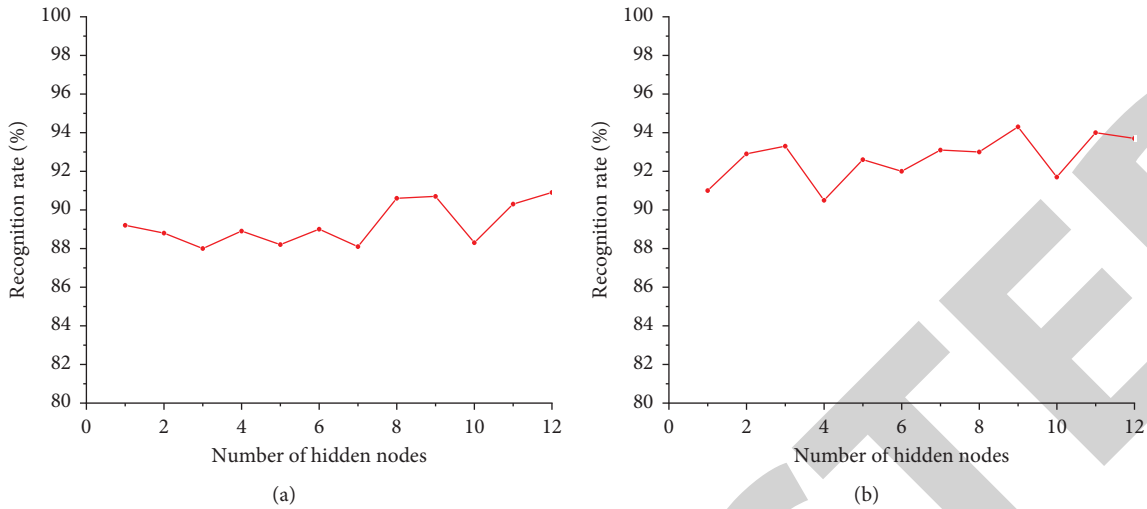


FIGURE 7: The recognition rate of the number of nodes in each hidden layer of the neural network. (a) Recognition rate of fist movement. (b) Recognition rate of palm valgus.

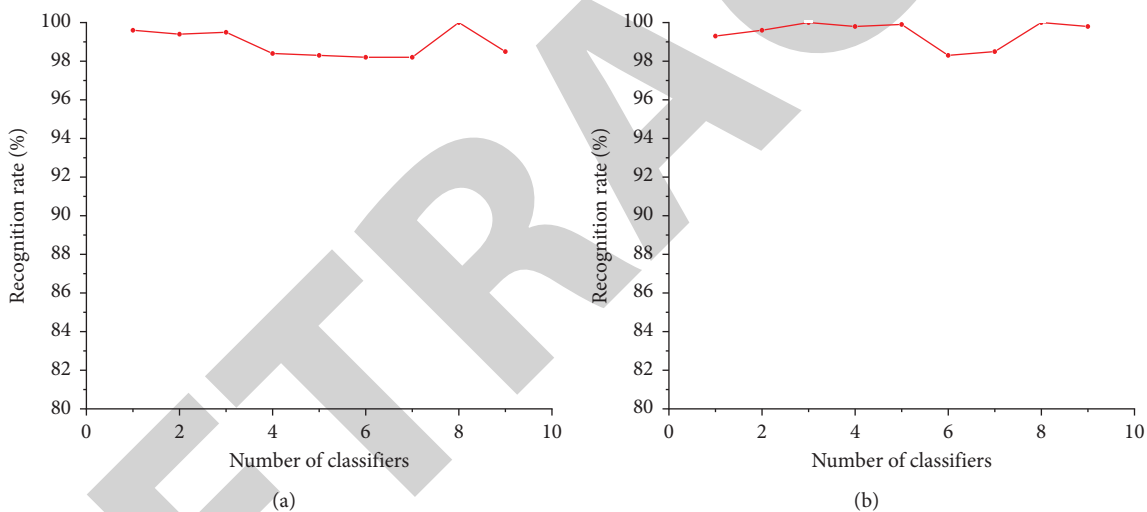


FIGURE 8: The recognition rate of the number of weak classifiers in the AdaBoost algorithm. (a) Recognition rate of fist movement. (b) Recognition rate of palm valgus.

this article presents the physical frame structure to realize the link, the outline design method of each signal processing unit in the transmitter and receiver [21]. Finally, this article introduces the detailed design method of each signal processing unit in the transmitter and receiver, and gives the interface definition and interface connection method. In the general design and detailed design part, the design methods of frequency domain notch, moment assist, and iterative interference suppression technology will be introduced.

Figure 10 shows the block error rate performance when the signal-to-noise ratio  $\text{SNR} = 4$  dB, interference signal priority detection, spread spectrum signal priority detection, and interference-free suppression. It can be seen that when the signal-to-noise ratio  $\text{SNR} = 4$  dB, the critical point of the block error rate performance of the interference

signal priority detection and the spread spectrum signal priority detection is about the interference signal ratio  $= 0.2$  dB. When the interference signal ratio is greater than the critical point, the block error rate (BLER) performance of the interference signal priority detection method is better than that of the spread spectrum signal priority detection method. When the interference signal ratio is less than the critical point, the BLER performance of the spread spectrum signal priority detection method is better than that of the interference signal priority detection method [22]. In addition, when the signal-to-noise ratio  $\text{SNR} = 4$  dB and the interference signal ratio  $\text{ISR} = -1$  dB, the BLER performance of the spread spectrum signal priority detection method is better than that of no interference suppression, and the block error rate performance is increased from 0.13 to 0.00042.

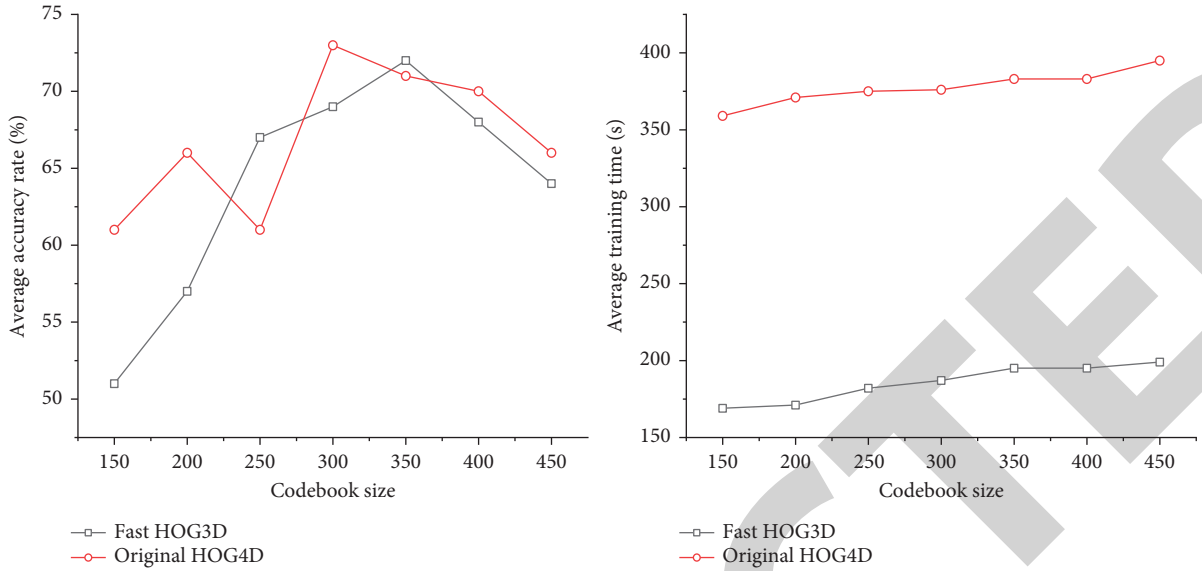


FIGURE 9: BoW-based recognition under different codebook sizes.

TABLE 4: Fixed-point simulation parameters of broadband digital interference scenarios.

Numbering	Parameter name	Parameter value
1	Frame length	10
2	Service rate	3.165
3	Encoding	LDPC
4	Modulation	QPSK
5	Spreading code	458
6	Spreading factor	6
7	Scrambling	65
8	Signal bandwidth	21.35
9	Signal intermediate	65
10	SNR	12
11	Frequency deviation	300
12	Broadband interference	21.35
13	IF carrier frequency	65

Human posture information has received more and more attention in current behavior recognition research, but image or video features are usually added as the main basis of behavior to reduce the effect of posture estimation results on the accuracy of behavior recognition. However, when selecting action features for expressing diversity, researchers often choose to use human actions to fuse underlying features such as colors, textures, and edges of data processing. Feature selection provides dynamic information for feature fusion in this case, because it rarely considers the relationship between different features and whether the use of features conforms to the current application context. The video processed by the interference suppression algorithm can identify the dance movements of the human body through multiple key frames [23].

This design only applies SFT technology to the capture process in the joint algorithm, and the main considerations are as follows. Since the SFT algorithm has steps such as rearrangement and down-sampling, if the SFT algorithm is used to simplify the algorithm in the narrowband

interference suppression module, it will cause the loss of useful signals when the interference correlation peak is eliminated. This makes the time-domain signal finally recovered by the subsequent capture module deviate greatly from the original signal. Therefore, SFT-based anti-jamming algorithms are more suitable for interference detection rather than cancellation. The signal restoration technology based on SFT needs further research. The interference model used in the interference suppression module in this design is simple strong single-tone interference. In future research, we can continue to explore the performance of the joint algorithm in multi-tone interference and time-varying narrowband interference environments, and seek the possibility of combining the algorithm with multi-band filters [24].

## 5. Discussion

This paper uses gesture-based methods to recognize video dance movements and mainly uses the method of continuous frames of human body posture joint position change trend to conduct video analysis, eliminate invalid movements, reduce the amount of calculation, and improve the efficiency of dance movement recognition. At the same time, this paper uses the time information in the continuity of dance movements and the change information of the actor's posture sequence to obtain the actor's movement and posture characteristics in the video, so as to achieve a higher recognition rate. This article still has the following problem: in this article, the video frame sequence will be split before the feature extraction is performed to obtain a small continuous sequence of different actions, and most irrelevant actions are screened out. However, there will still be highly repetitive information between the intra-class frames, and the action recognition will not be affected after the effective data frame extraction is performed on the intra-class action frames. The difficulty lies in the determination and selection of thresholds when extracting valid frames within a class,

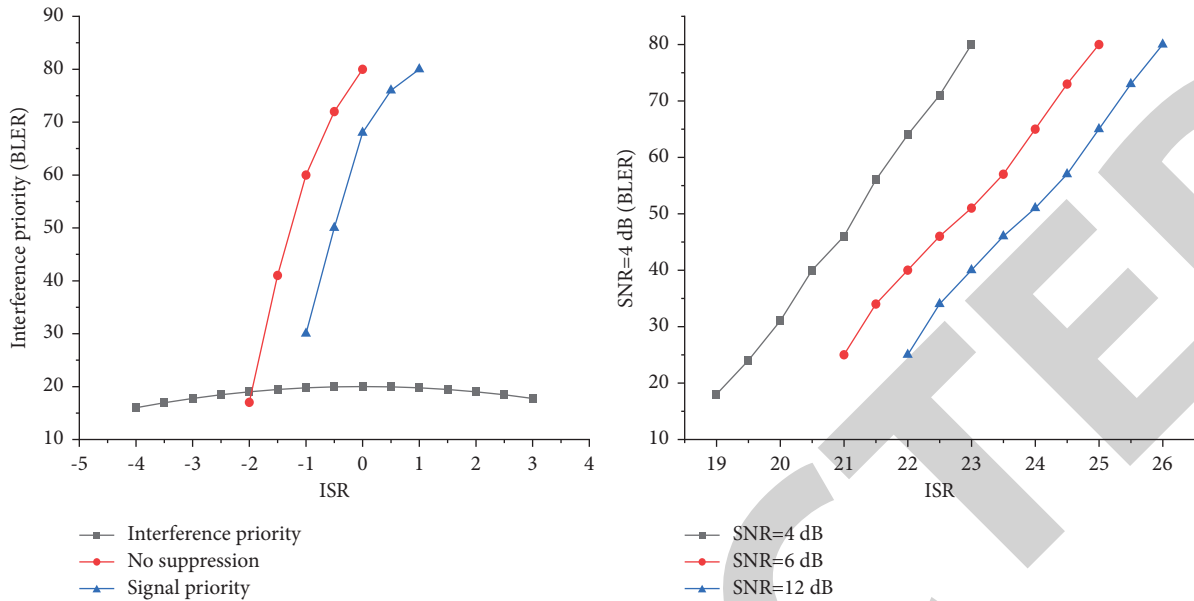


FIGURE 10: Performance comparison of block error rate under different iteration sequences under wideband interference.

and the thresholds between different types of actions are not the same. Although the use of SFT to simplify the Fourier transform of sparse signals can bring many benefits, its application scenarios are relatively limited, and it will also bring some problems that traditional methods do not have. It is worthy of further research and discussion in the future. In this paper, two features that contain static and dynamic information of actors and are complementary in function are selected as the main recognition features, and at the same time, gesture features are added to assist. Although it can be obtained by observing the experimental results that this method is superior to the method of combining characterization and dynamic features, this paper does not study in depth in the direction of feature fusion. Therefore, it cannot determine which feature combination method is more effective when fusing features in time-space, global-local, dynamic-dynamic, and other methods, nor can it be determined whether the fusion of more features can achieve a higher recognition rate [25, 26]. When using multiple features at the same time, it will face the problem of feature fusion weighting, and the choice of weights also has a certain impact on the final recognition result.

## 6. Conclusions

Contour model and AdaBoost algorithm technology have been applied to various industries, including human leisure and entertainment, medical treatment, intelligent monitoring, and other fields closely related to human life, as well as professional movement correction, folk dance, and other cultural relic movement records. Motion recognition research has been developed from simple behavior recognition to complex human behavior research in video. The current goal is to recognize the specific actions taken in the video. The next step is to recognize the purpose of the human body to perform certain types of actions. Most experiments use

support vector machines as the discriminator, but rarely use the AdaBoost algorithm. In order to study the performance of AdaBoost in behavior recognition, this paper designs a behavior recognition system based on hierarchical BP-AdaBoost. The experimental results prove the superiority of AdaBoost in terms of training time and recognition accuracy, and the hierarchical recognition framework can greatly reduce the training cost and the mixed slip between action classes, so that the recognition rate is significantly improved.

## Data Availability

No data were used to support this study.

## Disclosure

The author received no financial support for the research, authorship, and/or publication of this article.

## Conflicts of Interest

The authors declare that the research was conducted in the absence of any commercial or financial relationships that could be construed as potential conflicts of interest.

## References

- [1] N. Alipour and R. Hasanzadeh, "Superpixel-based brain tumor segmentation in MR images using an extended local fuzzy active contour model [J]," *Multimedia Tools and Applications*, vol. 80, no. 5, pp. 1–25, 2021.
- [2] X. Yang and X. Jiang, "A hybrid active contour model based on new edge-stop functions for image segmentation," *International Journal of Ambient Computing and Intelligence*, vol. 11, no. 1, pp. 87–98, 2020.
- [3] C. Feng, J. Yang, C. Lou, and W. K. D. Li, "A global inhomogeneous intensity clustering- (GINC-) based active contour model for image segmentation and bias correction,"

- Computational and Mathematical Methods in Medicine*, vol. 2020, no. 5, pp. 1-18, Article ID 7595174, 2020.
- [4] X.-C. Zhao, J. Z. Yuan, J.-Z. Yuan, and H.-Z. Liu, J.-S. Zhou, Improved AdaBoost algorithm for robust real-time multi-face detection," *Journal of Software*, vol. 12, no. 1, pp. 53-61, 2017.
- [5] Y. Liu, W. Tian, Y. Li, and H. Yang, "Fast CU termination algorithm with AdaBoost classifier in HEVC e," *IEICE - Transactions on Info and Systems*, vol. E101.D, no. 9, pp. 2220-2223, 2018.
- [6] J. Yang and D. Luo, "The P2P risk assessment model based on the improved AdaBoost-SVM algorithm," *Journal of Financial Risk Management*, vol. 06, pp. 201-209, 2017.
- [7] X. Yang, N. Liang, W. Zhou, and H. Lu, "A face detection method based on skin color model and improved AdaBoost algorithm," *Traitement du Signal*, vol. 37, no. 6, pp. 929-937, 2020.
- [8] A. Vard, "A new combination active contour model for segmenting texture image with low contrast and high illumination variations," *Multimedia Tools and Applications*, vol. 77, no. 15, pp. 20021-20042, 2018.
- [9] W. Chen, C. Liu, and B. Pan, "An improved active contour model based on local information," *OALib*, vol. 08, pp. 1-10, 2021.
- [10] A. Sharma, "Brain region segmentation using low MSE based active contour model and convolutional neural network," *International Journal of Advanced Trends in Computer Science and Engineering*, vol. 9, no. 2, pp. 1848-1853, 2020.
- [11] H. Zhang, G. Wang, Y. Li, and H. Wang, "Faster R-CNN, fourth-order partial differential equation and global-local active contour model (FPDE-GLACM) for plaque segmentation in IV-OCT image," *Signal, Image and Video Processing*, vol. 14, no. 3, pp. 509-517, 2020.
- [12] A. S. Abdullah, J. Rahebi, Y. E. Özok, and M. Aljanabi, "A new and effective method for human retina optic disc segmentation with fuzzy clustering method based on active contour model," *Medical, & Biological Engineering & Computing*, vol. 58, no. 1, pp. 25-37, 2020.
- [13] Y. Peng, S. Liu, Y. Qiang, and X. L. Wu, "A local mean and variance active contour model for biomedical image segmentation," *Journal of computational science*, vol. 33, no. APR, pp. 11-19, 2019.
- [14] O. Qun Wong and P. Rajendran, "Image segmentation using modified region-based active contour model," *Journal of Engineering and Applied Sciences*, vol. 14, no. 16, pp. 5710-5718, 2019.
- [15] G. Wang and G. Yang, "Facial expression recognition using PCA and AdaBoost algorithm," *International Journal of Signal Processing Systems*, vol. 7, no. 2, pp. 73-77, 2019.
- [16] C. Yan, Z. Wang, and C. Xu, "Gentle Adaboost algorithm based on multi-feature fusion for face detection," *Journal of Engineering*, vol. 2019, no. 15, pp. 609-612, 2019.
- [17] H. Zhou and G. Yu, "Research on fast pedestrian detection algorithm based on a neural network and AdaBoost," *Complexity*, vol. 2021, no. 6, 17 pages, Article ID 5548476, 2021.
- [18] C. Jiang, Y. Kang, C. Ye, and S. YU, "Applications of improved PSO\_BP\_adaboost algorithm in fault diagnosis of dimension out-of-tolerance," *Zhongguo Jixie Gongcheng/China Mechanical Engineering*, vol. 29, no. 20, pp. 2490-2494, 2018.
- [19] Y. Liu, J. Qiao, and L. Wei, "Research of preceding vehicle identification based on haar-like features and adaboost algorithm," *ICIC Express Letters*, vol. 12, no. 6, pp. 575-581, 2018.
- [20] J. Wan, L. Li, H. Yan, and W. A. N. G. ShaoHua, "An entity alignment approach based on the VS-Adaboost algorithm," *Beijing Huagong Daxue Xuebao (Ziran Kexueban)/Journal of Beijing University of Chemical Technology (Natural Science Edition)*, vol. 45, no. 1, pp. 72-77, 2018.
- [21] G. Sun, H. Tang, K. Lin, Y. Zhang, and D. Zhao, "Automatic fault recognition for key parts of train based on multi-feature fusion and BP-AdaBoost algorithm," *Zhongguo Jixie Gongcheng/China Mechanical Engineering*, vol. 28, no. 21, pp. 2588-2594, 2017.
- [22] A. Faridee, S. R. Ramamurthy, and N. Roy, "HappyFeet: challenges in building an automated dance recognition and assessment tool," *Mobile computing and communications review*, vol. 22, no. 3, pp. 10-16, 2018.
- [23] A. Fiskvik, "Renegotiating identity markers in contemporary hp," *Dance Research Journal*, vol. 52, no. 1, pp. 45-57, 2020.
- [24] S.-B. Tsai, Y. Xue, J. Zhang et al., "Models for forecasting growth trends in renewable energy," *Renewable and Sustainable Energy Reviews*, vol. 77, pp. 1169-1178, 2017.
- [25] S.-B. Tsai, "Using the DEMATEL model to explore the job satisfaction of research and development professionals in China's photovoltaic cell industry," *Renewable and Sustainable Energy Reviews*, vol. 81, pp. 62-68, 2018.
- [26] S.-B. Tsai, J. Yu, L. Ma et al., "A study on solving the production process problems of the photovoltaic cell industry," *Renewable and Sustainable Energy Reviews*, vol. 82, pp. 3546-3553, 2018.